COMMISSIONING A SPECTROGRAPH FOR THE LEUSCHNER 30-INCH TELESCOPE

A thesis presented to the faculty of
San Francisco State University
In partial fulfilment of
The Requirements for
The Degree

Master of Science
In
Physics with a Concentration in Astronomy

by

Audrey Frances Dijeau

San Francisco, California

June 2019

CERTIFICATION OF APPROVAL

I certify that I have read *COMMISSIONING A SPECTROGRAPH FOR THE LEUSCHNER 30-INCH TELESCOPE* by Audrey Frances Dijeau and that in my opinion this work meets the criteria for approving a thesis submitted in partial fulfillment of the requirements for the degree: Master of Science in Physics with a Concentration in Astronomy at San Francisco State University.

Ronald Marzke
Professor of Physics and Astronomy

Adrienne Cool
Professor of Physics and Astronomy

Joseph Barranco
Associate Professor of Physics and Astronomy

COMMISSIONING A SPECTROGRAPH FOR THE LEUSCHNER 30-INCH TELESCOPE

Audrey Frances Dijeau
San Francisco State University
2019

This thesis details the commissioning of the Shelyak Instruments Littrow High Resolution Spectrograph (LHIRES III) for use on the Leuschner 30-inch telescope in Lafayette, California. The commissioning of this new instrument included the installation of a Starlight Xpress "Ultrastar" imaging and guiding camera, and an SBIG ST-8300 CCD Camera on the unit. Installation of the device was completed in May 2019, and the commissioning of the device was completed in June 2019. Additionally, this thesis contains a guide and demonstration of how to use the device and how to reduce spectra using IRAF.

I certify that the Abstract is a correct representation of the content of this thesis.

6/25/2019

Chair, Thesis Committee   Date

ACKNOWLEDGMENTS

The years I've spent at San Francisco State University have been a journey. I could fill volumes with the amount of kindness I have received since starting as an undergrad here and through my time as a grad student, so if you have touched my life, thank you.

First, thank you to my parents for supporting me all these years as I pursued this path.

Second, thank you to the SFSU Symphony Orchestra. I'm so happy that I have been able to grow as a musician as I have grown as an astronomer.

Finally, thank you to the people in the Physics and Astronomy Department. I could not have done this without your guidance, kindness, and support. Thank you to the Women in Physics and Astronomy Club, and to all the people I've shared this journey with on the first floor of Thornton Hall. Thank you Caroline Alcantara for always being there when I've needed help. Thank you Jim Gibson for all your help at Leuschner and at the SFSU Observatory. Thank you to the professors who have supported me over the years, including Chris McCarthy and Kim Coble. And of course, an astronomically large thank you to my thesis committee: Adrienne Cool, Joe Barranco, and Ron Marzke.

Ron, your mentorship means the world to me. Thank you for believing in me.

TABLE OF CONTENTS

LIST OF TABLES

LIST OF FIGURES

Chapter 1

Introduction

1.1 History of The Leuschner Observatory

The Students' Observatory, which opened in Fall 1887, was originally founded for civil engineering students at the University of California, Berkeley. The observatory eventually separated from the Department of Civil Engineering and Astronomy when the Berkeley Astronomical Department was created [13].

In 1892, Armin Otto Leuschner began as an instructor of astronomy courses at The Students' Observatory [13]. He was appointed as the first director of the Berkeley Astronomical Department, and the observatory now bears his name [2].

While the observatory was originally located on the UC Berkeley campus, it was relocated in 1965 to the Russell Reservation, 10 miles east of Lafayette, CA [2].

1.2 The Thirty Inch Telescope

The Leuschner 30-inch telescope was accepted from Tinsley Laboratories in February 1968 [10]. The telescope is of a Ritchey—Chrtien design, has an effective focal length of 240 inches, and has a nominal f-ratio of 8 [1]. Ritchey—Chrtien telescopes have a deeply concave hyperboloid shaped primary mirror, and a secondary mirror which is a steep convex hyperboloid. These features allow the telescope to produce clear images with large fields of view [11].

Figure 1.1: The 30-inch Telescope at the Leuschner Observatory in Lafayette, CA.

The 30-inch Telescope was recollimated in 2001 by graduate students at The University of California, Berkeley [1].

In 2009, San Francisco State University partnered with the UC Berkeley to refurbish the Leuschner 30-inch telescope. The telescope's drive motors and control systems were upgraded in 2012. Descriptions of the control systems may be found in the theses of Adam Fries and Eileen Gonzales, former graduate students at SFSU [5] [6]. The telescope was equipped with an SBIG STL-11000 CCD camera for imaging [19].

The telescope is currently used by students from UC Berkeley and SFSU. Students from SFSU make trips to the observatory for astronomy classes, and also operate the telescope and imaging camera remotely from an observing station on the SFSU campus.

1.3 Spectra

In 1814, Joseph von Fraunhofer cataloged 475 dark lines in the solar spectrum. Fraunhofer determined that the wavelength of one prominent dark line in the Sun's spectrum corresponded to the wavelength of the light emitted when salt is sprinkled in a flame [3]. In the discovery and identification of this sodium line, Fraunhofer created the new science of spectroscopy.

Light that we receive from objects in space generally includes a large number of wavelengths. With traditional imaging, we see the sky as our eyes see it, with all wavelengths of light overlapping each other. While we are able to use filters to limit which wavelengths we image at once, a filter does not allow the examination of the different wavelengths themselves. For this, we can use a device to separate the light according to wavelength, and thus image the spectrum of wavelengths of light that we are receiving from an object.

In 1860, Gustav Kirchhoff and Robert Bunsen published *Chemical Analysis by Spectral Observations*, in which they presented the idea that each element has its own unique pattern of spectral lines, and by observing these unique spectral lines, you would be able to identify each element.

Kirchhoff summarized the production of spectra with three laws: A hot dense gas or solid object produces a continuous spectrum, a hot diffuse gas produces bright spectral emission lines, and a cool diffuse gas in front of a continuous spectrum source produces dark absorption lines in the continuous spectrum [3].

An object's continuous, or blackbody, spectrum can be used to determine an object's temperature. The blackbody spectrum of a hot dense gas or solid object of temperature T peaks at a wavelength λ_{max}. The relation between λ_{max} and T is Wien's displacement law [3]:

$$\lambda_{\text{max}} T = 0.002897755 \text{ m K}. \tag{1.1}$$

The emission lines of a hot, diffuse gas are created when an electron in an atom transitions down from a higher energy level to a lower energy level and emits a photon with an energy equal to that which was lost in the electron's transition. In other words, $E_{\text{photon}} = E_{\text{high}} - E_{\text{low}}$. The energy of a photon is related to its wavelength, and also its momentum, p, in the following manner [3]:

$$E_{\text{photon}} = h\nu = \frac{hc}{\lambda} = pc. \tag{1.2}$$

The wavelengths of the absorption lines of a cold, diffuse gas in front of a continuous spectrum source are similarly determined by the energy levels available to an electron the atoms of an element. Characterizing energy levels to be "orbits" such as those in the Bohr model, we can say "when an incident photon in the continuous spectrum has exactly the right amount of energy, equal to the difference in energy between a higher orbit and the electron's initial orbit, the photon is absorbed by the atom and the electron makes an upward transition to that higher orbit" [3].

The uniqueness of the spectral lines is due to which orbitals may be occupied by electrons. The Pauli exclusion principle says that no two electrons can share the same quantum state. Which orbitals are occupied by electrons depends on the temperature, density, and pressure of its environments, so these, as well as other things such as the strength of a surrounding magnetic field, may also be determined by examining spectral lines [3].

In addition to spectra being a tool to discern chemical composition, you can also observe the Doppler shifts of stellar spectral lines to determine the radial velocity of a star with the following relation:

$$\frac{\lambda_{\text{obs}} - \lambda_{\text{rest}}}{\lambda_{\text{rest}}} = \frac{\Delta\lambda}{\lambda_{\text{rest}}} = \frac{v_r}{c}, \tag{1.3}$$

for $v_r << c$ [3].

1.4 Spectrographs and Spectroscopy

The device that we use to turn the light we receive from a source into a spectrum is called a spectrometer. A spectrograph is a spectrometer which also has an imaging device to record the spectrum. Generally, a spectrograph is attached to a telescope in place of an eyepiece or other imaging device.

In a spectrometer, the light from the observed object first travels through a narrow slit. The slit blocks out light from other parts of the sky, and additionally restricts the image in a particular dimension so that the spectral lines of one part of the image do not overlap any other spectral lines. The narrower the slit, the higher the resolution of the spectrograph, but the dimmer the image will be. The angular size of the slit on the sky is

$$\phi_s = \frac{w_s}{f_{\mathrm{TEL}}}, \tag{1.4}$$

where w_s is the slit width and f_{TEL} is the focal length of the telescope. The slit must be placed in the focal plane of the telescope.

After traveling through the slit, the light is diverging and must be passed through a collimating lens. The collimator lens turns the light into a set of parallel rays.

The f-ratio of the collimator must be close to that of the telescope, where

$$\text{f-ratio} = \frac{\text{focal length}}{\text{diameter}}. \tag{1.5}$$

After going through the collimator, the now collimated beam of parallel light rays strikes a dispersing element at an angle β with the normal. A diffraction grating can either be a transmission grating, which light can pass through, or reflection grating, from which the separated wavelengths of light will be reflected. A transmission grating is comprised of a series of slit like openings, while a reflection grating is a series of narrow mirrors or facets. Grating facets are a distance d apart, called the groove spacing. The grating equation is

$$\alpha = \sin^{-1}\left(\frac{m\lambda}{d} - \sin\beta\right), \tag{1.6}$$

where m is the order, and α is the angle at which the wave is reflected or diffracted. When the incoming light is normally incident on the grating, we can derive the simple expression

$$d\sin\alpha = m\lambda. \tag{1.7}$$

For large numbers of facets, any rays that do not satisfy the grating equation are suppressed by interference effects [4].

The spectrometer's ability to resolve wavelengths separated by $\Delta\lambda$ is given by

$$\Delta\lambda = \phi_s \frac{D_{\text{tel}}}{D_{\text{col}}} \frac{d}{m} \cos\beta, \tag{1.8}$$

where D_{tel} is the diameter of the telescope, and D_{col} is the diameter of the collimating lens [4].

The ratio $R = \lambda/\Delta\lambda$ is the resolving power of the grating [3]. Generally, spectrographs with $R < 1,000$ are considered low resolution, $1,000 < R < 10,000$ medium resolution, and finally, $R > 10,000$ high resolution.

After the light has been diffracted by the dispersing element in the spectrograph, the light goes through a camera lens which focuses the rays onto a detector, such as a CCD camera. The spectrum is recorded by the detector.

Chapter 2

New Instruments for the Leuschner 30-inch Telescope

2.1 Shelyak Instruments Littrow High Resolution Spectrograph

The Shelyak Instruments Littrow High Resolution Spectrograph (LHIRES III) was acquired by the Physics and Astronomy Department at SFSU. This spectrograph has both a guiding hole and a spectrum imaging hole.

The spectrograph uses a mirrored slit, which should be positioned at the focal plane of the telescope. The mirrored slit is mounted on a removable slit holder, which allows for easy removal and cleaning. If the slit is not clean, light from the target object may be blocked. We recommend removing dust from the slit with compressed air.

Figure 2.1: LHIRES III Spectrograph installed on the Leuschner 30-inch telescope, with the SBIG ST-8300 (right) and the "Ultrastar" (left) CCD cameras attached and powered on.

Light that does not go down the slit is reflected and sent through the guiding hole. Light that does go through the slit is bounced off a flat 45° mirror and is then sent through the spectrograph's collimator, which has a focal length of 200 mm and a 30 mm diameter. The collimated beam travels to the reflection grating, which is mounted on a support which can be rotated by adjusting a micrometer screw on the outside of the spectrograph to examine different ranges of wavelengths.

The LHIRES III has a grating holder which may be switched out to use gratings of various rulings. Both a 2400-line and 300-line grating were purchased, however, the 300-line grating was not used in this project and will not be discussed further in this thesis. The manufacturer specified the 2400 lines per millimeter holographic grating as part of the nominal configuration of the spectrograph. A holographic grating is etched using lasers rather than using a cutting tool on the surface of the grating. The use of a holographic grating has benefits such as greater precision and lower surface scattering when compared to a ruled grating produced with a cutting tool [4]. The manufacturer states that spectral dispersion given by this grating is 0.114 Å/pixel in the red.

The user guide provided by the manufacturer stated that the resolving power of this spectrograph, with a slit width of 25 μm and over a linear 8 mm field, is around 17,000 in the red, allowing the spectrograph to resolve details smaller than 0.4 Å around the hydrogen alpha line [9].

	LHIRES III with 2400 line per millimeter grating
Dispersion (around Hα)	0.12 Å/pixel
Resolving Power	17000
Limiting Magnitude	5.0
Spectral Range	85 Å

Table 2.1: Spectrograph parameters given by the manufacturer for a 200 mm f/10 telescope, 30 μm slit, and a KAF0400 camera [9].

The ideal input focal ratio for the spectrograph is f/10, and the acceptable range is between f/8 and f/12 [9]. This range is inclusive of the f-ratio of the Leuschner 30-inch telescope, which is f/8.

We used the 2400 lines per millimeter holographic grating, along with a slit of width 23 μm.

Figure 2.2: Reflective four position slit on the slit holder. The 15,19, 23, and 35 μm slits and their labels are visible in the image.

The LHIRES III was mounted to the 30-inch telescope using a custom adapter machined at SFSU. The adapter was installed on the device in the place of the telescope interface provided by the manufacturer. The adapter allows the LHIRES III to be securely bolted onto the back of the 30-inch telescope in a position where the focal plane of the telescope intersects with the slit.

2.2 SBIG ST-8300 CCD Camera

We are using the SBIG ST-8300 CCD camera as our spectrum imaging camera. The camera is mounted to the spectrum imaging hole of the spectrograph.

The SBIG ST-8300 uses a Kodak KAF-8300 CCD with a 3326 × 2504 pixel array [7]. The device was installed directly onto the spectrograph and positioned so that the spectrum image would be projected along the long, horizontal axis of the device.

CCDOPS was used as our camera control software. This software is made for computers running Windows and is provided for free on the camera manufacturer's website[1]. The spectral range we recorded with this CCD camera was around 301 Å, with a dispersion of approximately 0.09 Å/pixel.

Figure 2.3: SBIG ST-8300 CCD camera on the back of a telescope.

[1]CCDOPS may be downloaded from Diffraction Limited's Legacy Product Support page, located at https://diffractionlimited.com/support/sbig-archives/ [14].

2.3 Starlight Xpress "Ultrastar" Imaging and Guiding Camera

We are using the Starlight Xpress "Ultrastar" imaging and guiding camera to image the light bouncing off the reflective slit through the guiding hole. The "Ultrastar" guide camera was installed with an eyepiece adapter which was inserted into the guiding hole. The adapter allowed the guide camera to be in a position where an image of the slit was in focus. Once the image of the slit is in focus, the guide camera is in the proper position and should not be moved. The focus of the telescope may then be adjusted using the image from the guide camera.

We used Starlight Live to control the guide camera, as well as to view a live feed of images coming from it. Starlight Live is a free software provided by the manufacturer of the CCD camera [2]. This software is available for computers running Windows and Mac OSX. The field of view of the camera is 3.8' $\times$ 5.2'. The guide camera was rotated until the image of the slit was horizontal in the guide camera image.The approximate length of the slit in the guide camera, measured from Figure 2.5, is $3.5'$. The width of the slit in the image was four pixels, or approximately $0.9''$. This is close $0.8''$, the theoretical value of the angular slit width calculated from the physical size in micrometers of the slit and the focal length of the 30-inch telescope.

[2]Starlight Live may be downloaded from Starlight Xpress ltd's Download page, located at https://www.sxccd.com/drivers-downloads [15].

Figure 2.4: Starlight Xpress "Ultrastar" Imaging and guiding camera [16].

Figure 2.5: Image of the field of view of the "Ultrastar" guide camera with the slit visible in the center of the image captured using Starlight Live. The telescope was pointed at the dome which was being illuminated by a halogen lamp.

Chapter 3

Using the Spectrograph

An observer should proceed on their observing run with the steps outlined here.

3.1 Starting Up

Start up the main Leuschner telescope control GUI (`xobs`) on the desktop computer at the observatory and turn on the power to the telescope and the dome[1]. The `xobs` program will be used to open and close the dome and mirror shutters, as well as point the telescope.

Connect the SBIG-8300 CCD camera power cable to the SBIG-8300 camera and an available power outlet. There is a power strip which is attached to the back of the telescope and turns on and off with the telescope power. The camera should turn on when plugged in to a powered outlet. Open CCDOPS on a laptop. Use

[1]Eileen Gonzales and Adam Fries include an explanation of how to operate the Leuschner telescope controls in their theses [5] [6].

the USB cable to connect the already powered CCD camera to the laptop. Use the CCDOPS software to begin communication between the CCD camera and the laptop. Turn on the cooling. During testing, the cooling was set to 5°C.

On a separate laptop, start Starlight Live. Connect the "Ultrastar" guiding camera USB cable to both the camera and the laptop and use the software to start communication between the two. The "Ultrastar" does not require an additional power source.

Choose which wavelengths you want to observe, and position the grating by turning the micrometer. To observe the zero order line, the micrometer should be set close to 0 mm. We found from our test observations that 15.28 mm is a good position to observe the magnesium triplet.

3.2 Flat Field Images

Flat field images are useful for removing the pixel-to-pixel variations in sensitivity of pixels on the CCD in science images. The observer must obtain flat field images for each wavelength range observed.

Generally, the observer would take sky flats, dome flats, and internal flats. There is not currently an internal lamp to be used in the LHIRES III. Sky flats will include the solar spectrum and telluric contamination. Dome flats should be made with light sources which provide a continuous spectrum.

For sky flats, images should be taken of the blue sky, before twilight. The slit drastically limits the light which gets to the spectrum imaging camera, which causes signal to noise ratio to become increasingly poor as sunset approaches.

Dome flats can be obtained, but because the mirror shutters and the dome are connected and one cannot normally be opened without the other, power must be cut to the dome to open the mirror shutters without opening the dome. There is a halogen lamp at the observatory which may be aimed at the wall. The telescope is aimed at the illuminated wall and an image is taken to make a dome flat.

3.3 Darks and Bias

For each science image exposure time, you should take a dark image with the same exposure time. The darks should also be taken with the camera set to the same temperature as it was during the science image exposures, as the dark current is dependent on temperature. Dark images can be taken through the CCDOPS software, which will close the camera shutter for you.

CCDOPS will not allow exposure times of less than 0.090 seconds to be made. This is an obstacle in taking 0 second bias images. However, the dark images also contain the bias so we merely subtracted the darks from our images, knowing that the bias is also being subtracted.

3.4 Reference Spectra

Reference spectra are important for the wavelength calibration of your science images. An image of the spectrum from a lamp which emits lines of known wavelengths must be made in order to determine which pixel in an image corresponds with each wavelength.

There are several gas tubes (currently neon, helium, and mercury) and a power supply at the observatory which may be used to obtain reference spectra. To image the light from these tubes, we pointed the telescope at a wall and manually held up the lamp which we wanted to use, shining the light directly into the telescope. An exposure of at least 60 seconds is necessary for a reasonable signal to noise ratio.

Reference spectra images should be taken before and after each object in order to account for any movement of the grating.

3.5 Imaging the Object

The pointing of Leuschner is not perfect, and you may need to slew around using the paddle in `xobs` until the target object is in the field of view of the guide camera. This is made simple with Starlight Live, as it allows the guide camera to continually take images as you move the telescope around. We found that moving the telescope North (up on the paddle) moved objects to the left of the guide camera image, and moving West (left on the paddle) moved objects towards the bottom of the image.

The correction we used when taking science images of our target objects was -24.5 seconds in right ascension, and -1' 23" in declination. Making this adjustment to the RA and Dec of the target object allowed us to consistently get our targets in the field of view upon slewing to the object. See Appendix D for a list of objects observed successfully with this correction.

Once the target object is in the field of view of the guide camera, the telescope should be moved until the target object is on the slit. This will allow the light from the object to enter the slit and go through the spectrograph. Make sure to focus the telescope before imaging your object. We had success with focus values around 24,000.

3.6 Shutting Down

Use the software to disconnect both cameras. Unplug the cameras and turn off the laptops. Shutdown the telescope using `xobs` on the desktop computer at the observatory, and leave the desktop computer on.

Chapter 4

Image Reduction

Image Reduction and Analysis Facility (IRAF) is a useful tool to reducing spectra, and includes various packages to do so. There are many guides available on how to use IRAF to do this. A User's Guide to Reducing Slit Spectra with IRAF by Massey, Valdes, and Barnes (1992) is a useful place to start [17][1].

Here, we present a sample of an image reduction done on a spectrum from the star Vega. Our images were obtained with the SBIG ST-8300 CCD camera. To run IRAF tasks, we used PyRAF, a product of the Space Telescope Science Institute, which is operated by AURA for NASA. We installed PyRAF with Ureka.

[1]This document was previously available on the NOAO website, but is no longer on that site. I was able to find it at other URLS, including http://www.astro.iag.usp.br/~jorge/aga5802/spect_iraf_reducao.pdf [17].

4.1 Raw Images

We present in this section a selection of raw images obtained exported from SAOImage DS9. The micrometer position on the spectrograph was 15.28 mm, which enabled us to observe the magnesium triplet in both the sky flats and the Vega spectrum.

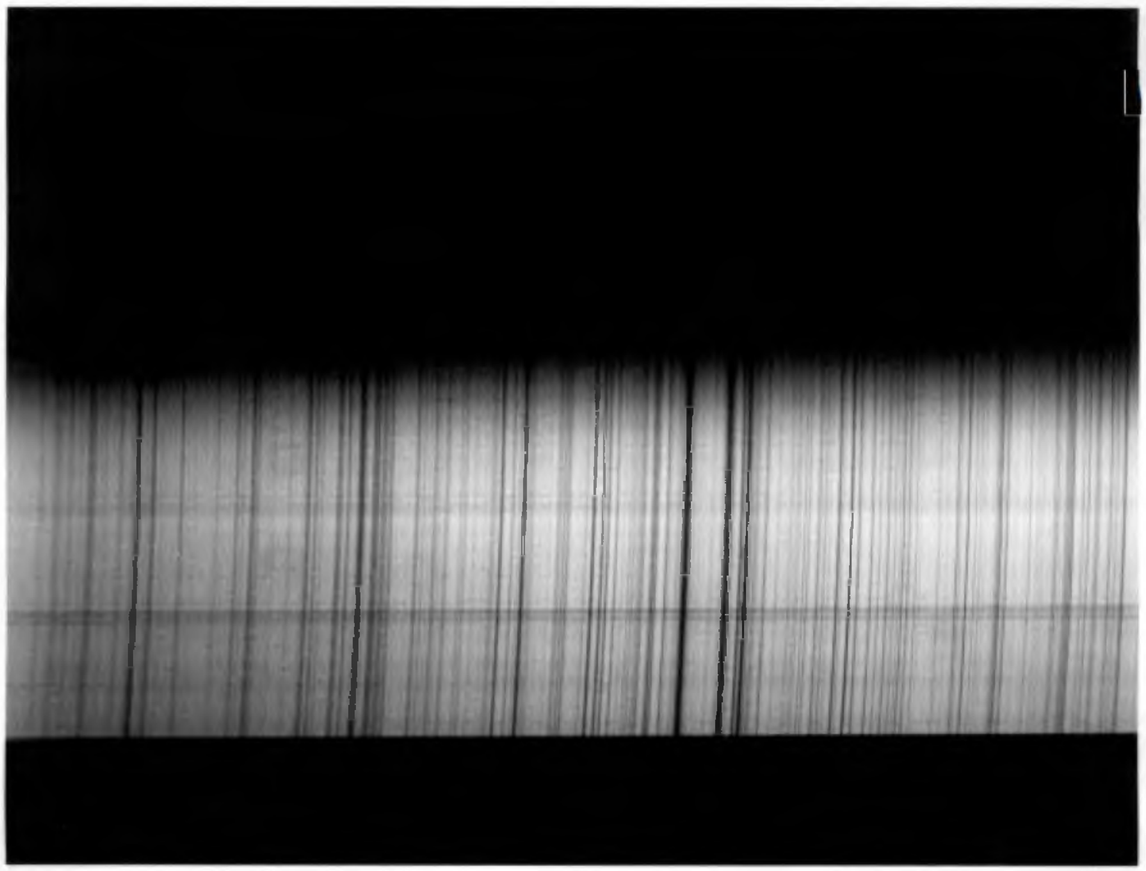

Figure 4.1: 120 second exposure of the sky on June 6, 2019 at 8:40 pm PDT. DS9 scale parameters: Low = 1285.5026, High = 2200.7883

Figure 4.2: 120 second exposure of light from a neon lamp. DS9 scale parameters: Low = 1025.0002, High = 3622.6566

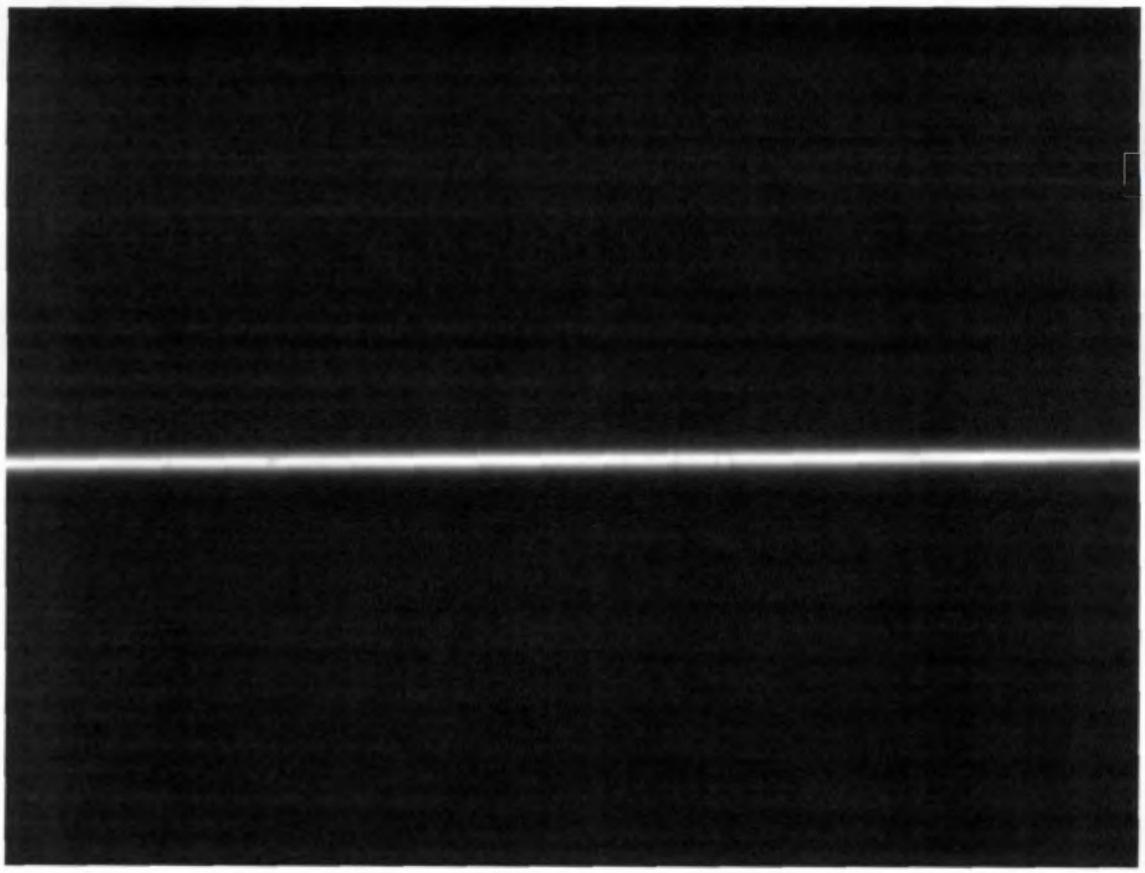

Figure 4.3: 60 second exposure of light from Vega on June 7, 2019 at 2:17 am PDT. DS9 scale parameters: Low = 1025.0002, High = 3622.6566

4.2 Dark Subtracted Images

We present here the dark subtracted images of a combined sky flat, one of our reference spectra, and our science image. We did not do a flat field reduction with these images.

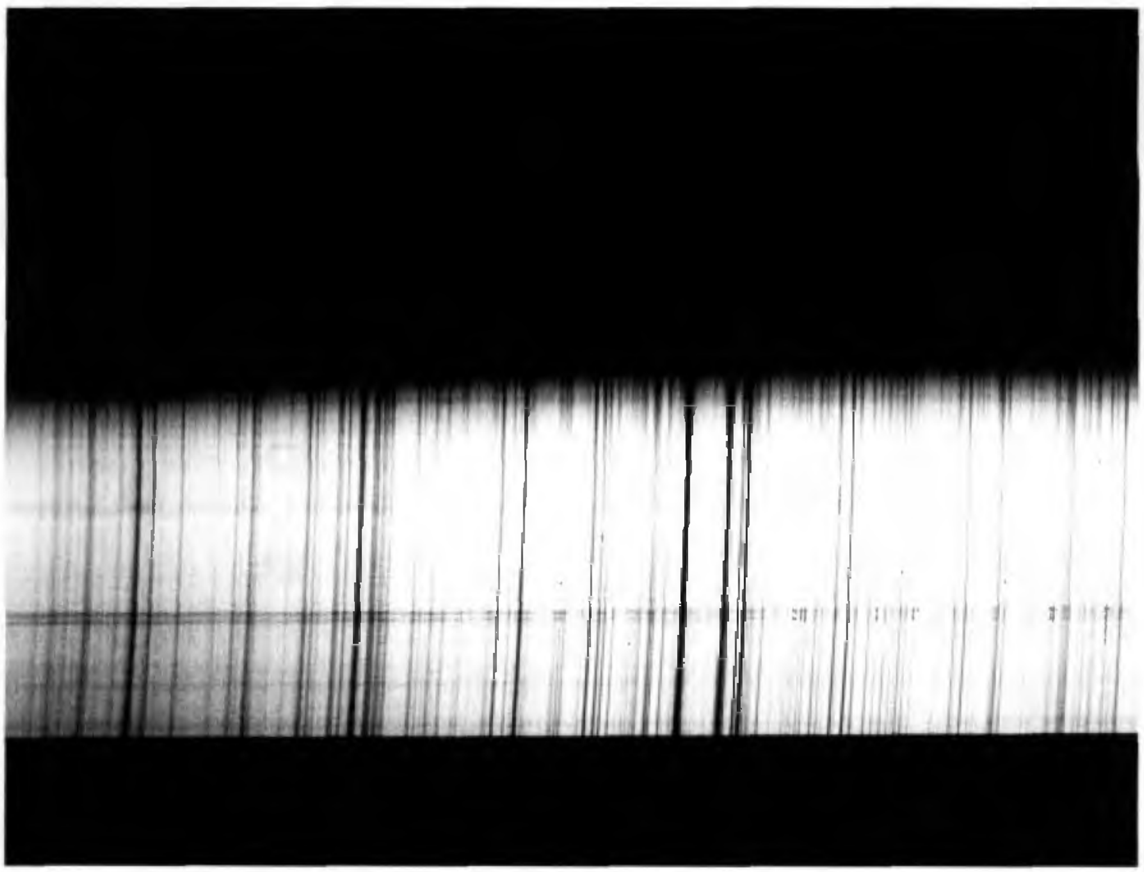

Figure 4.4: Sky flat made with a combination of two 60 second and two 120 second exposures. The images were dark subtracted before being combined. Note that the darks used for subtraction was taken with the CCD at a different temperature. DS9 scale parameters: Low = -164.4707, High = 561.46487

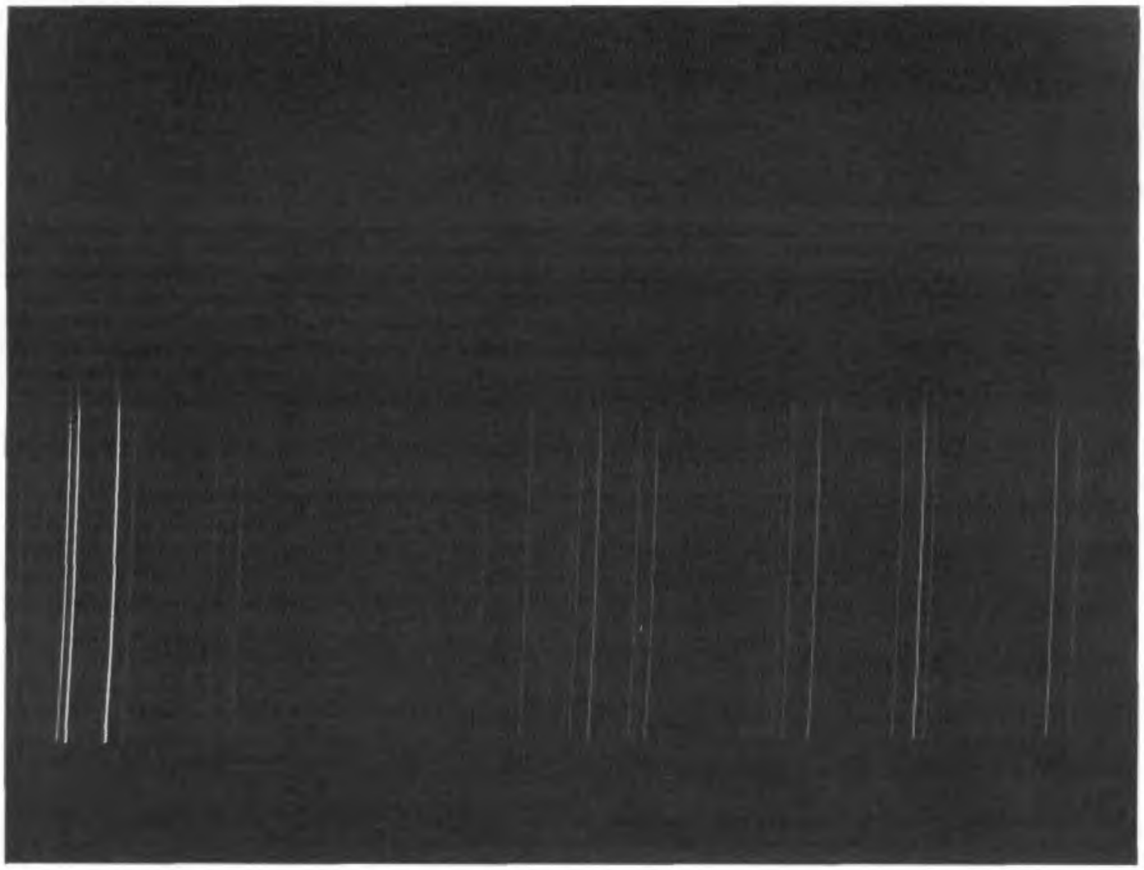

Figure 4.5: A dark subtracted 120 second exposure of a neon lamp. DS9 scale parameters: Low = -1085.3316, High = 1283.3329

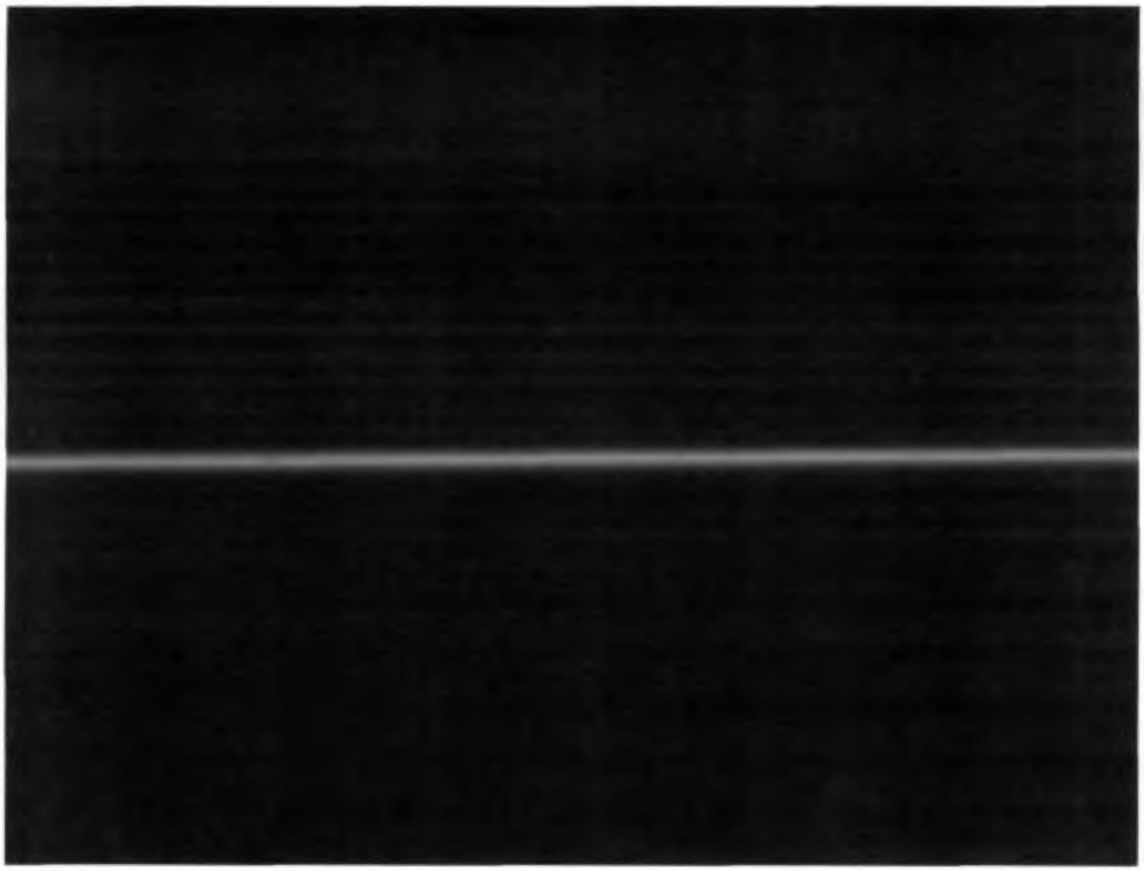

Figure 4.6: A dark subtracted 60 second exposure of Vega. DS9 scale parameters: Low = -5034.667, High = 40756.832

4.3 Extracted Spectrum

Here we present the extracted spectrum from our science image. Figure 4.7 indicates the aperture and background apertures selected for extraction. The aperture indicates which rows of pixels in the image will be extracted to have their columns summed to create a plot of the spectrum. Background apertures allow the sky to be subtracted from the spectrum. Aperture selection was accomplished with the `apall` task.

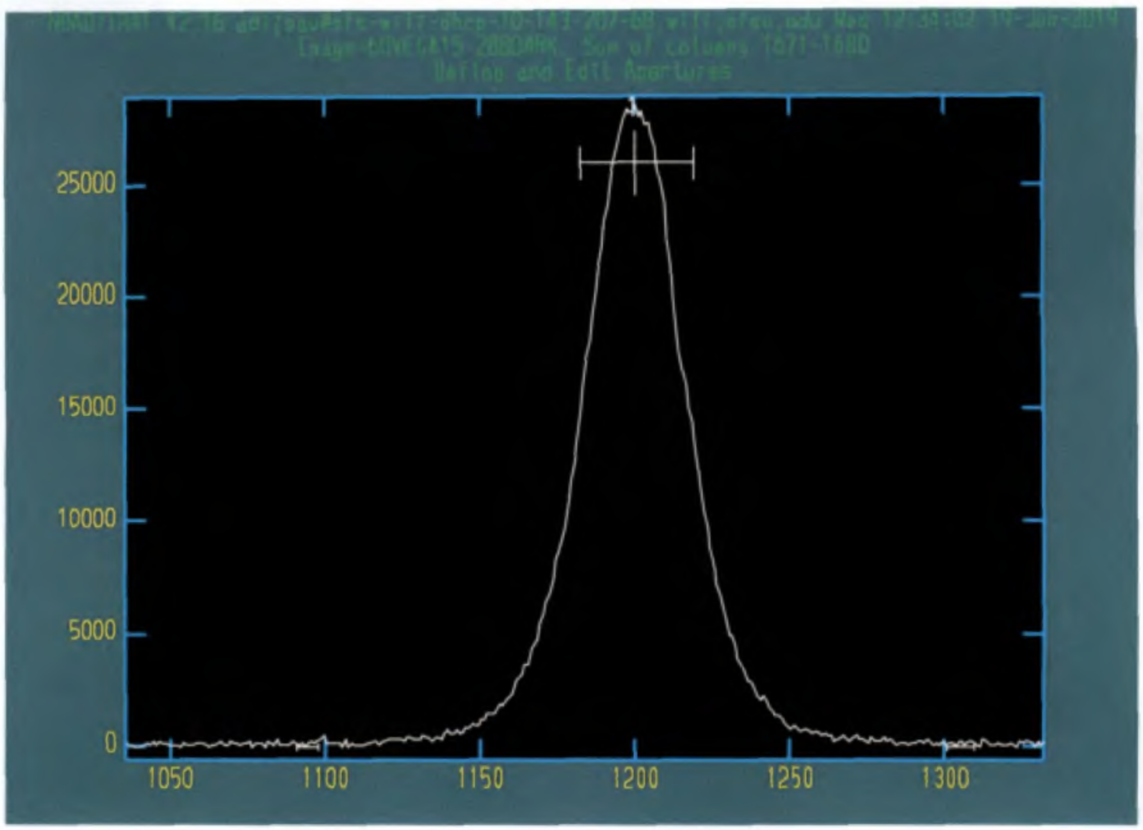

Figure 4.7: Selecting apertures to be used in extracting the spectrum. In this case, the x-axis lists pixels on the y-axis of the image, and the y-axis is counts. The source aperture is the large aperture centered around 1197 pixels. The two smaller apertures near 1100 and 1300 pixels are background apertures.

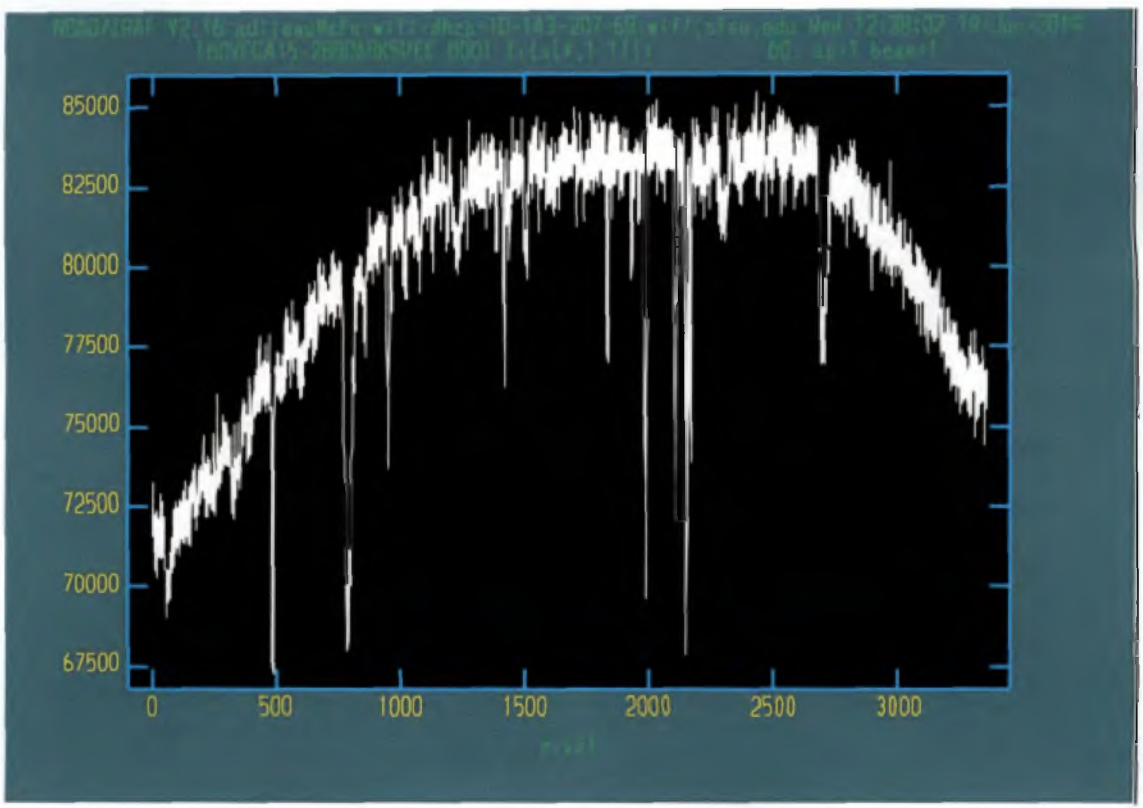

Figure 4.8: Extracted spectrum of dark subtracted image of a spectrum from Vega. (Counts vs Pixel)

We can see in our extracted spectrum prominent lines at 1980 pixels, 2102 pixels, and 2162 pixels, which would appear to be the magnesium triplet lines with wavelengths 5183.619 Å, 5172.698 Å, and 5167.327 Å, respectively.

The source aperture of our science image was then used as the aperture for our sky flat and our reference spectra.

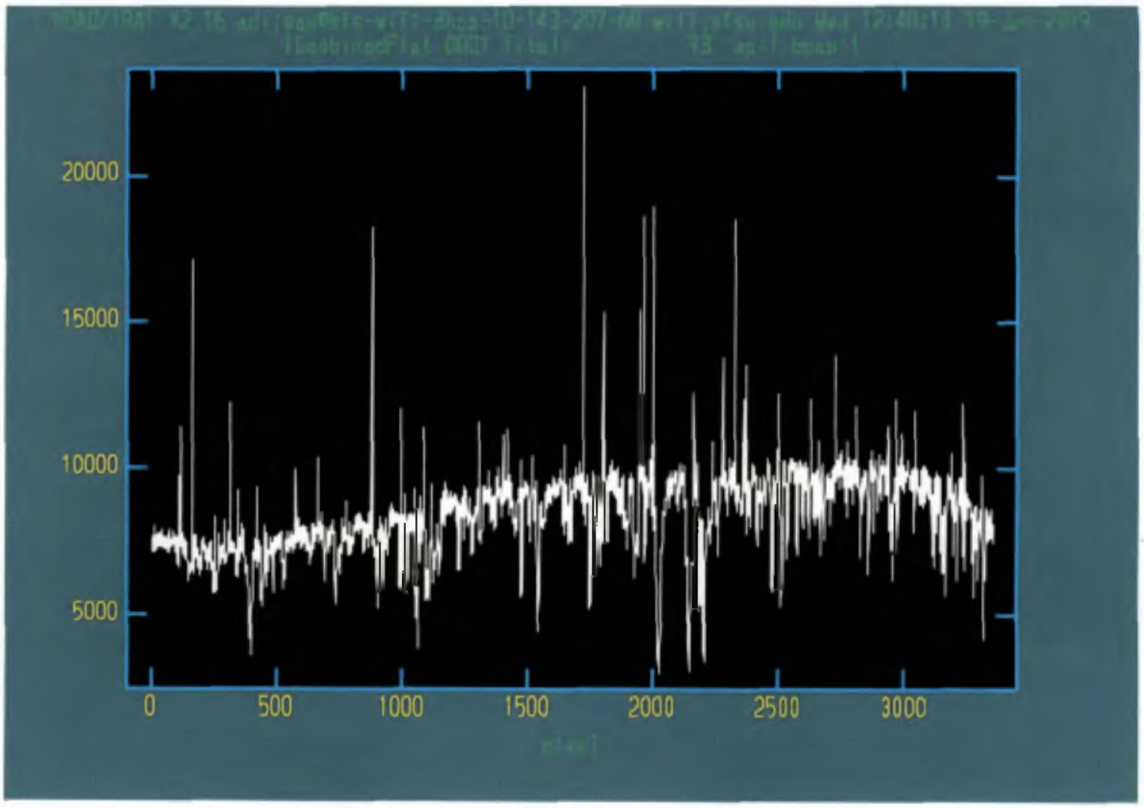

Figure 4.9: Extracted spectrum of the dark subtracted combined sky flat. (Counts vs Pixel)

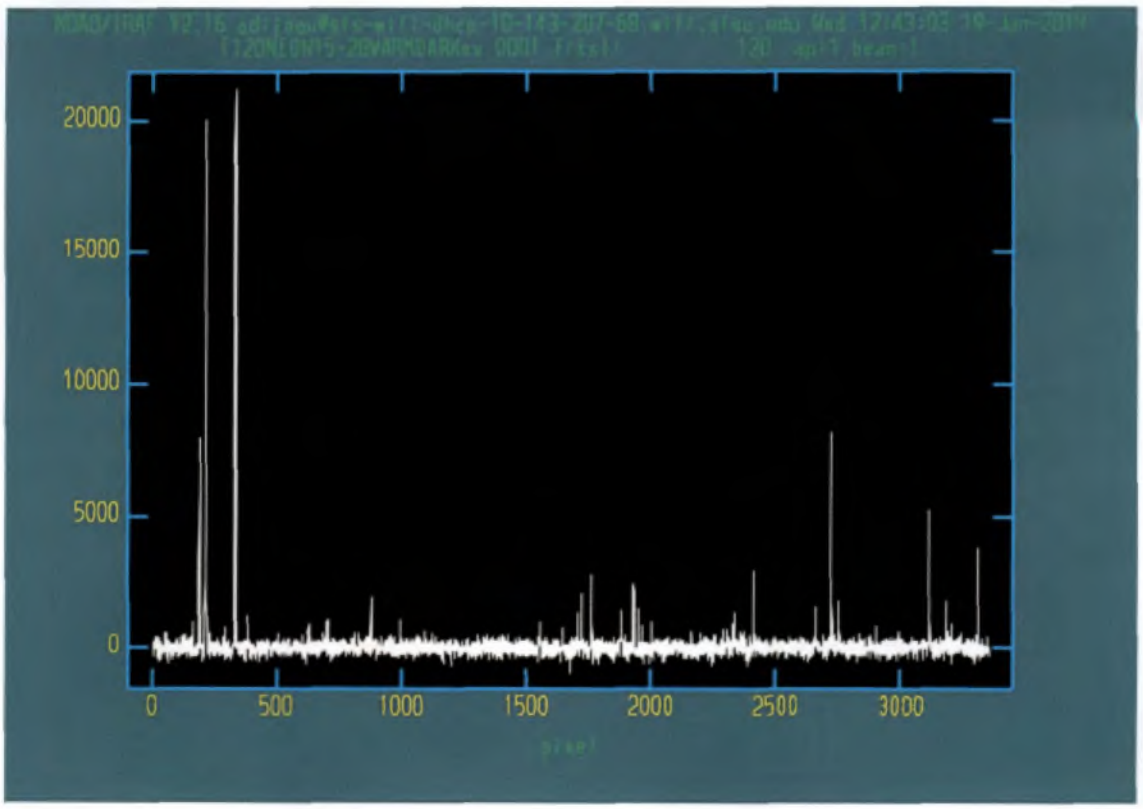

Figure 4.10: Extracted spectrum of 120 second exposure of light from a neon lamp. (Counts vs Pixel)

4.4 Wavelength Calibration

In order to present a spectrum as a function of wavelength rather than as a function of its pixel coordinates on the image captured, you need to calibrate the spectrograph for wavelength. To wavelength calibrate a spectrograph we must obtain a dispersion solution.

To do this you use a light source with known wavelengths and shine it into the spectrograph and into the slit. Next, you look at the image obtained from that light and identify which pixel each center of each known line falls on. You then fit a function, typically a polynomial, to this data. See Appendix A for the IRAF database files describing the dispersion solutions.

The `identify` task was used first on the sky flat, where the magnesium triplet was clearly visible. We used a line list containing a selection of bright lines from *The Solar Spectrum 2935Å to 8770Å: Second Revision of Rowland's Preliminary Table of Solar Spectrum Wavelengths* [18]. See Appendix C for samples of the data files we used with the `identify` task.

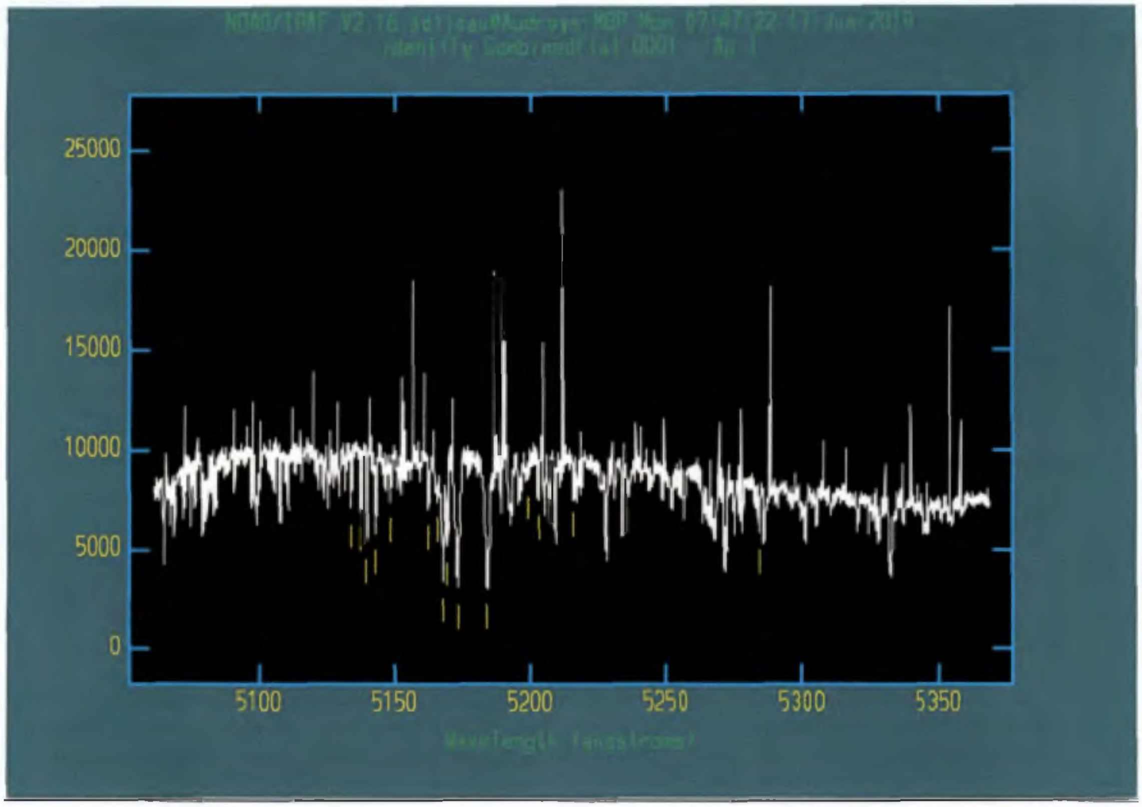

Figure 4.11: Wavelength calibrated sky flat. (Counts vs λ)

The sky flat was then used as a reference spectrum on the 120 second exposure of the neon spectrum. This was to make identifying the neon lines easier, since we were most certain in our identification of the magnesium triplet. To identify these lines, we used a list of neon lines between 5059 Å and 5360 Å retrieved from the NIST Atomic Spectra Database (see Appendix C) [12].

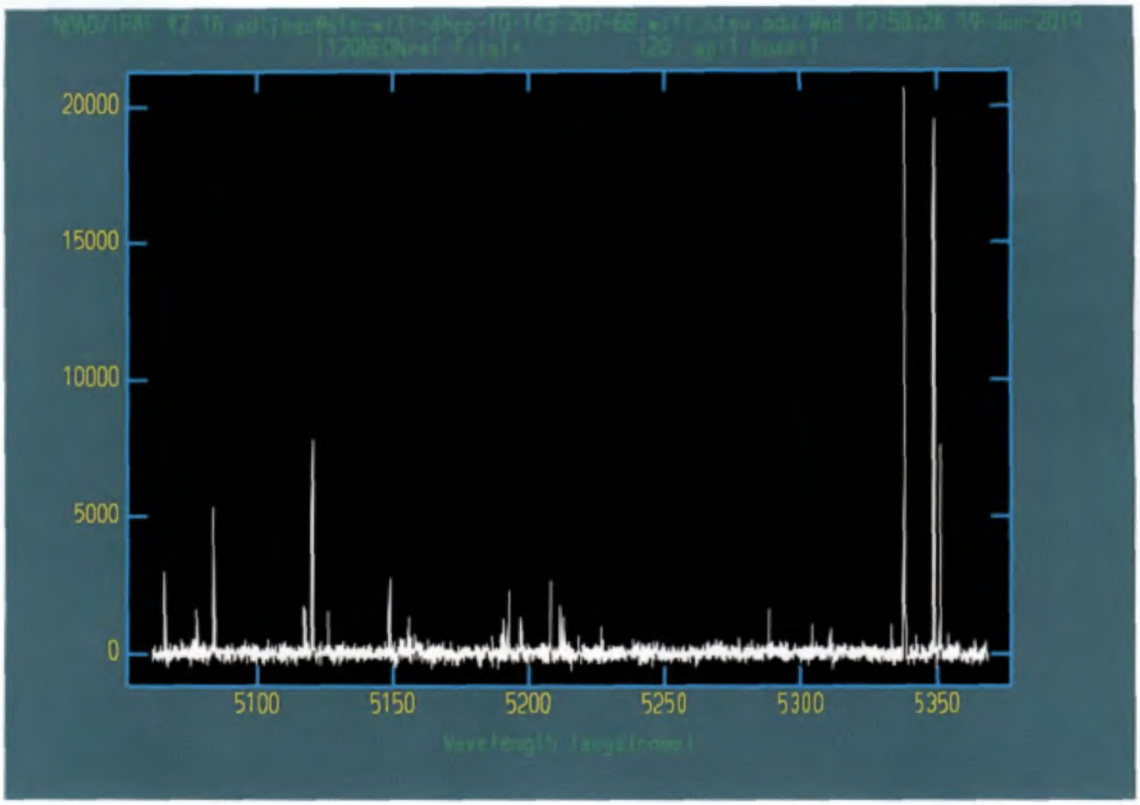

Figure 4.12: Wavelength calibrated neon spectrum. (Counts vs λ)

The 120 second exposure of neon was used as a reference spectrum and the `reidentify` task was used on two comparison neon spectra which were taken before and after our science image. These two comparison spectra were specified in the header of our Vega image and were used to run the `dispcor` task on the spectrum, completing the wavelength calibration for our spectrum.

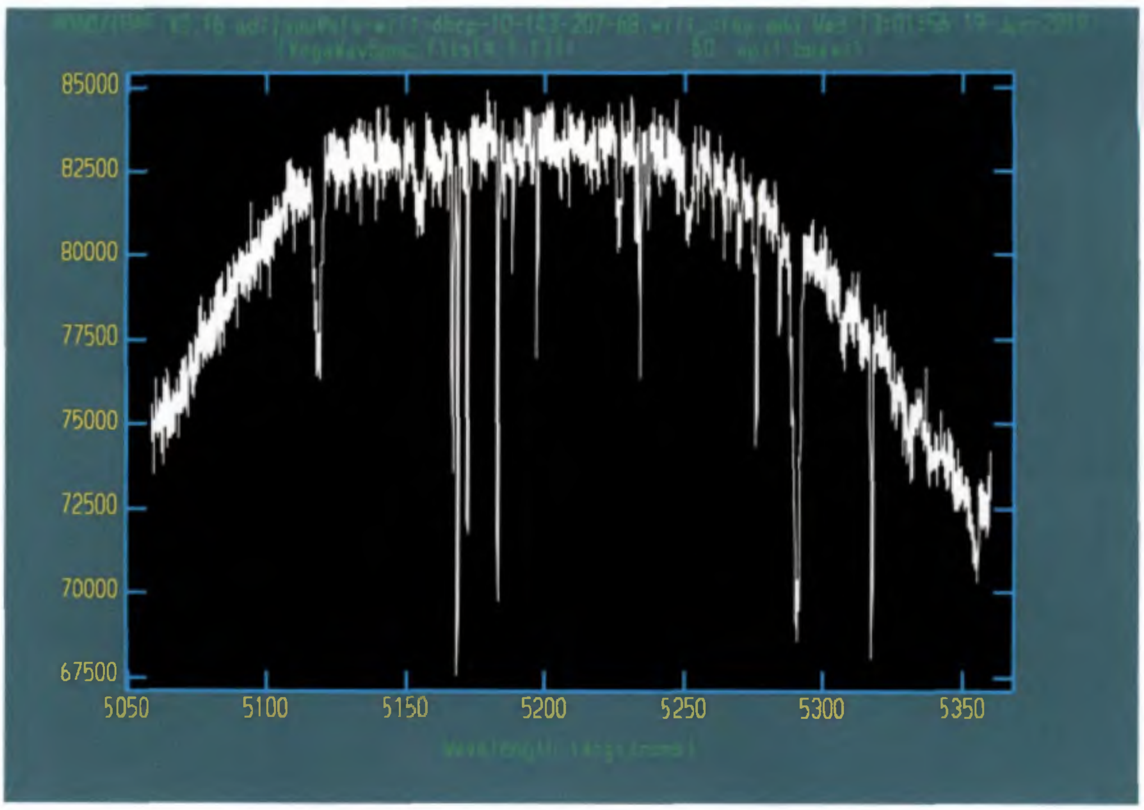

Figure 4.13: Wavelength calibrated spectrum of Vega. (Counts vs λ)

4.5 Flux Calibration

Flux calibration must be performed to present a spectrum in terms of flux units rather than counts.

We set the airmass close to 1 and included the atmosphere in the overall sensitivity measurement. No extinction correction was applied. Since Vega serves as a primary reference star for commonly used spectrophotometric systems, we can use our spectrum of Vega to calibrate our flux scale. We used a table of fluxes for different wavelengths of light from Vega, with 25 Å bins, from *Stellar Absolute Fluxes and Energy Distributions from 0.32 to 4.0 μm* by D. S. Hayes with the `standard` task to output a listing of counts within each bandpass (see Appendix C) [8].

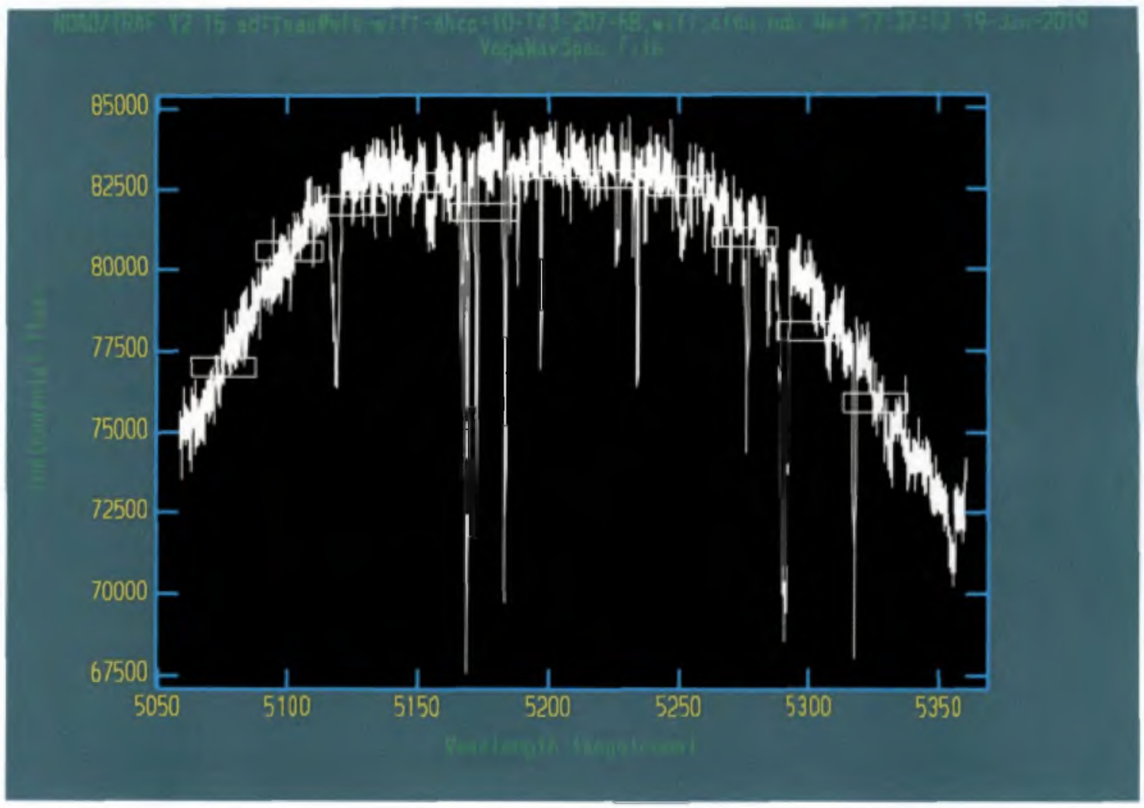

Figure 4.14: Viewing the bandpasses to do the flux calibration. (Counts vs λ)

We used the **sensfunc** task and selected a 5th order Chebyshev model to fit the sensitivity function. See Appendix B for the sensitivity function output from IRAF.

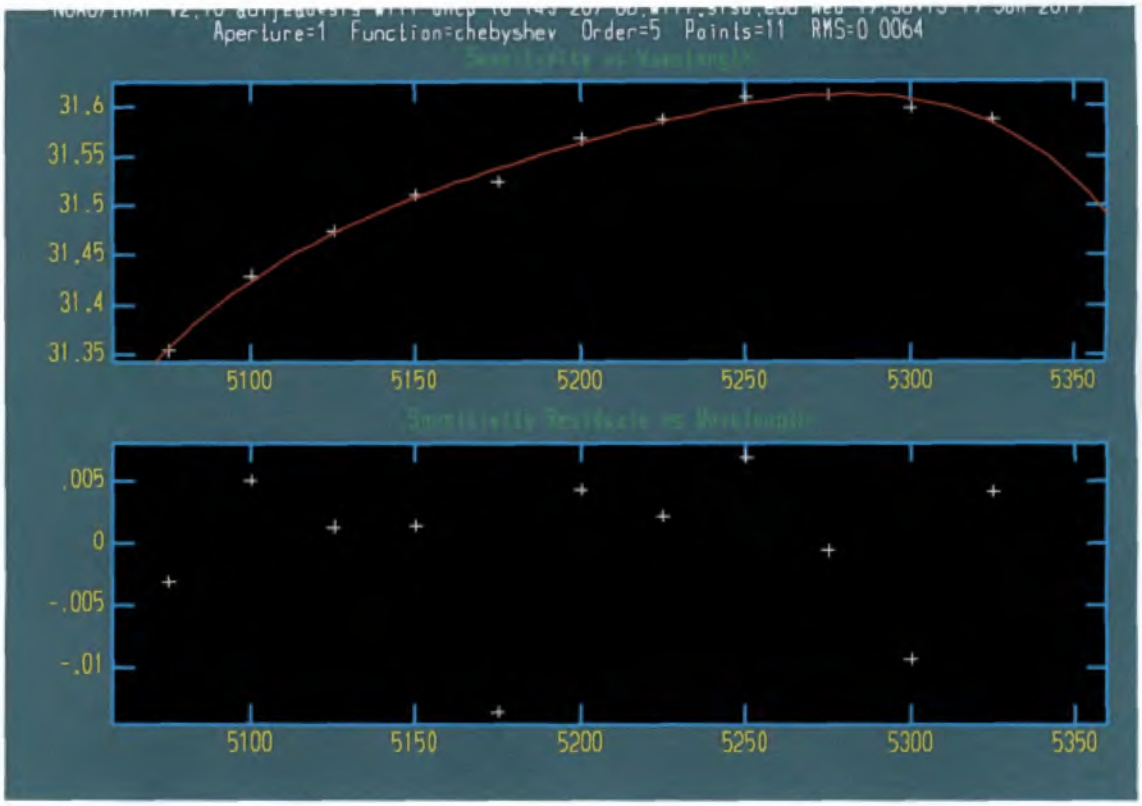

Figure 4.15: Fitting the sensitivity function as a function of wavelength.

The `calibrate` task was then used to complete the flux calibration.

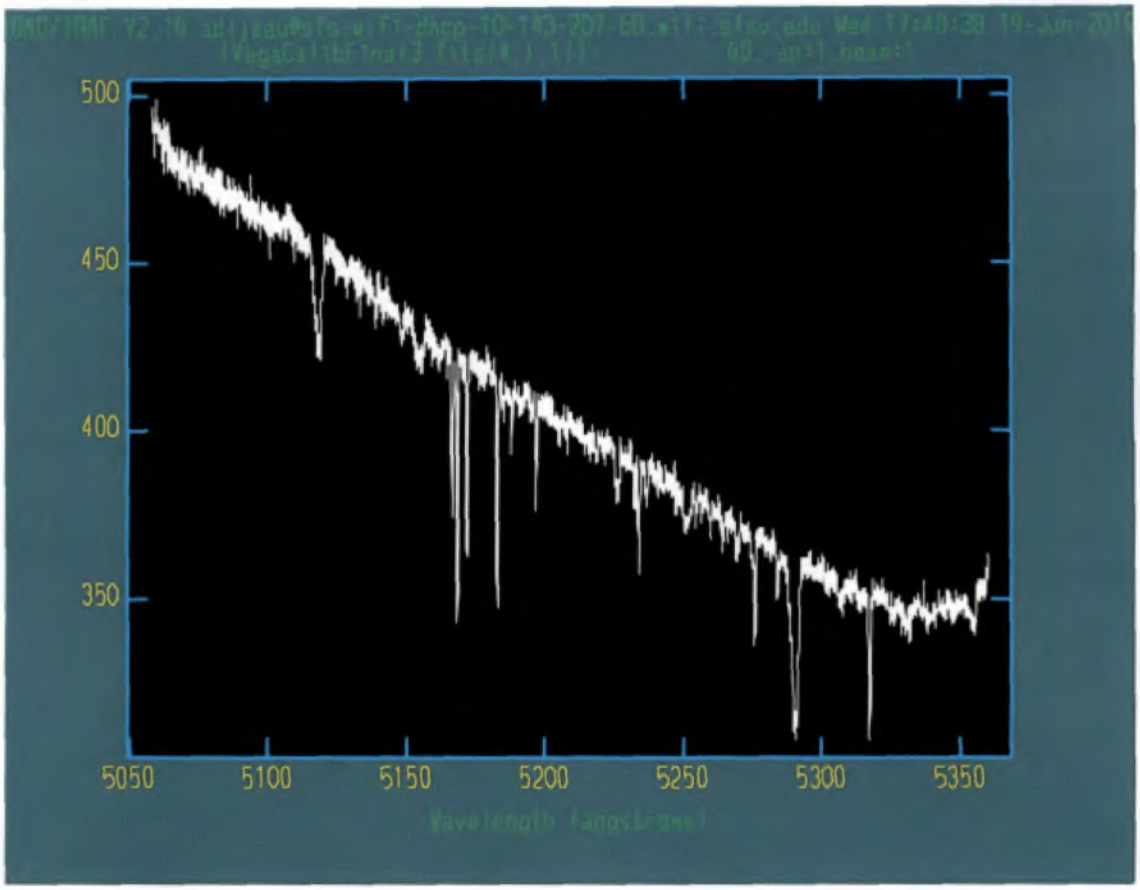

Figure 4.16: Flux calibrated spectrum of Vega (f_λ vs λ).

Note that past 5325 Å, our function is not fitted well. This is because wavelengths past that length are outside of the last bandpass which was used for our model.

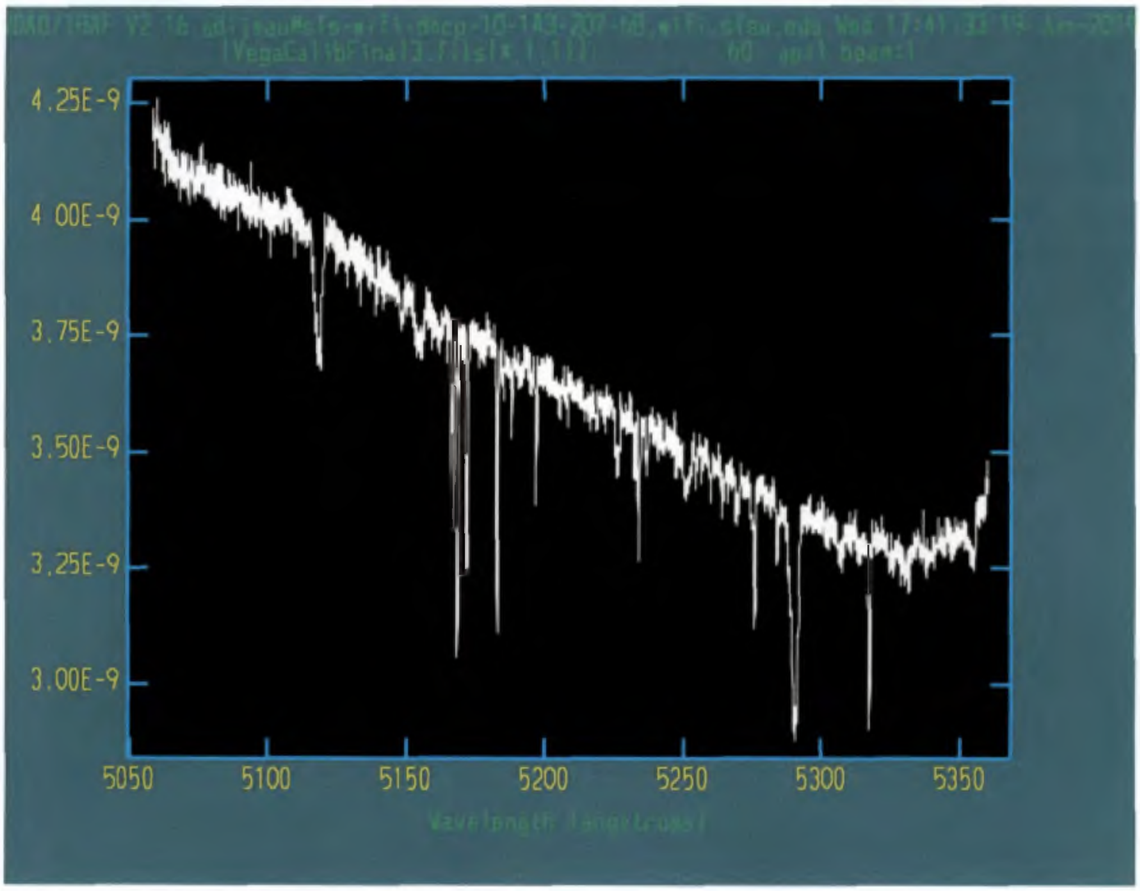

Figure 4.17: Flux calibrated spectrum of Vega (f_ν vs λ).

4.6 Normalized Calibrated Spectrum

We used a 10th order Chebyshev model and the `continuum` task to normalize the flux calibrated spectrum to the continuum. The normalized spectrum does not have the same fitting issue as the flux calibrated spectrum, and so has a somewhat larger wavelength range.

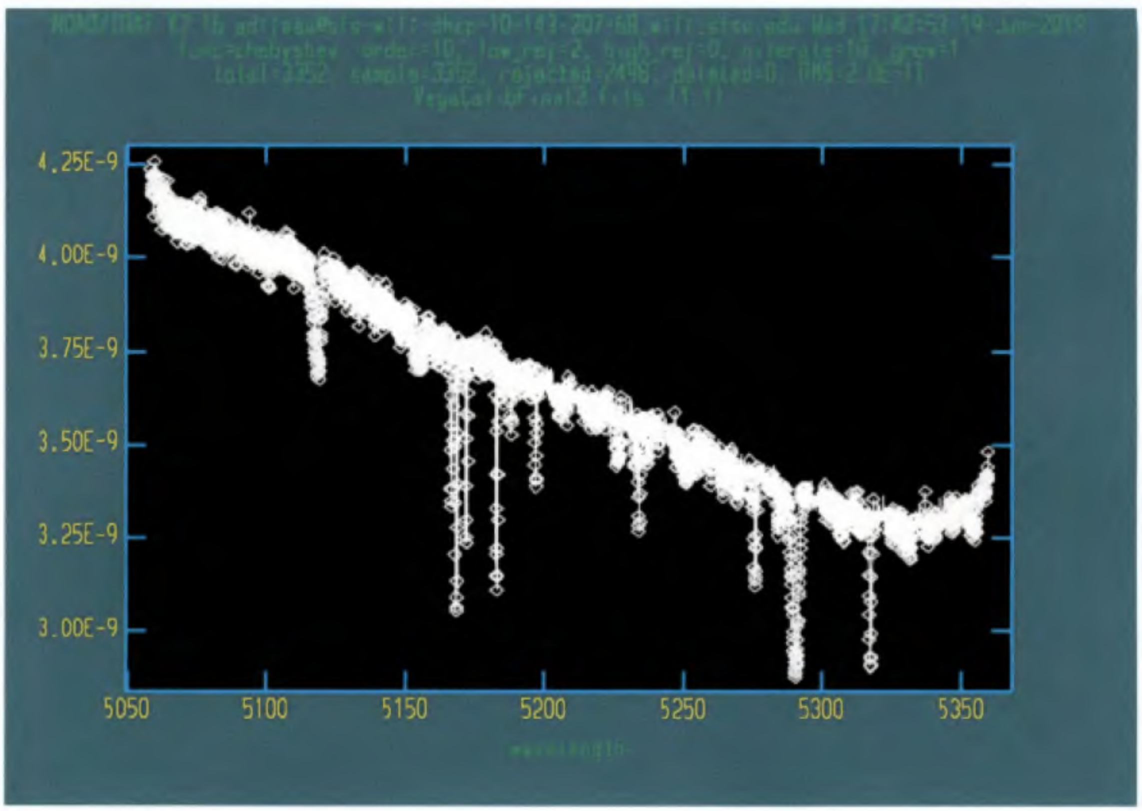

Figure 4.18: Fitting the normalization function.

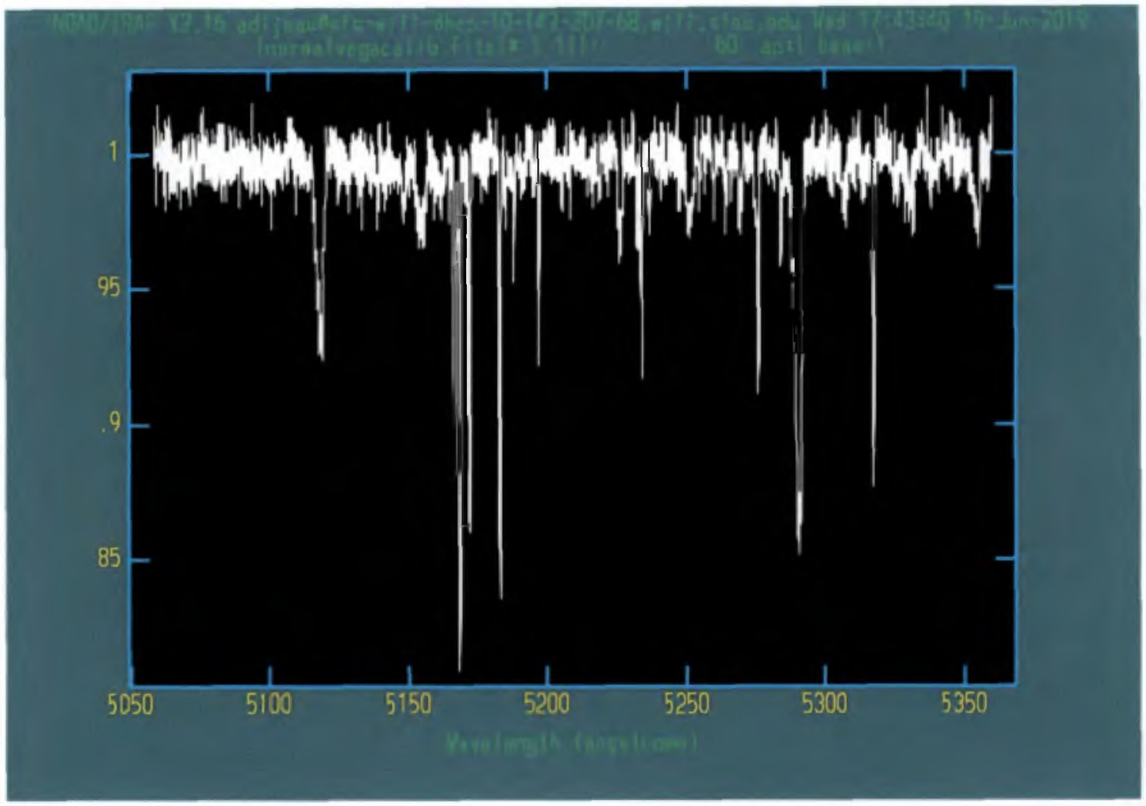

Figure 4.19: Normalized flux calibrated spectrum of Vega.

We can clearly see the magnesium triplet at 5166.522 Å, 5171.748 Å, and 5182.673 Å. Also note that this spectrum contains telluric contamination and shows lines from absorption in the Earth's atmosphere.

Comparing our measured wavelength values for the magnesium triplet to our known values for the magnesium triplet (5167.327 Å, 5172.698 Å, and 5183.619 Å), we see that there is approximately a 1 Å difference between the wavelengths given by our dispersion solution and the wavelengths we should observe. The uncertainty in the wavelength solution, with our dispersion of 0.09 Å/pixel, is significantly less than 1 Å. The primary source of this ~1 Å difference was the radial velocity of Vega with respect to our spectrograph at the time of observation.

Chapter 5

Spectrograph Parameters on the Leuschner 30-inch telescope

	LHIRES III with 2400 line per millimeter grating
Dispersion	0.09 Å/pixel
Spectral Range	300 Å
Guide Camera Field of View	3.8' × 5.2'
Slit Length in Guide Camera	3.5'
Slit Width in Guide Camera	0.9"
Dispersion Solutions	See Appendix A
Sensitivity	See Appendix B

Table 5.1: Spectrograph parameters for the Leuschner 30-inch f/8 telescope, 23μm slit, the SBIG ST-8300 CCD camera used as our spectrum imaging camera, and the Starlight Xpress "Ultrastar" used as our guiding camera.

	Signal to Noise for LHIRES III observing Vega
Exposure Time	60 seconds
Apparent Magnitude	0
S/N Ratio (splot)	145
Average Counts	83333
Gain	0.37e-/ADU
S/N ratio (calculated)	238

Table 5.2: Signal to noise ratio for the LHIRES III spectrograph observing Vega. Observations made using the Leuschner 30-inch, f/8 telescope, 2400 line per millimeter grating, 23μm slit, and the SBIG ST-8300 CCD camera.

Chapter 6

Future work with the LHIRES III and the Leuschner 30-inch Telescope

The LHIRES III enables students at SFSU and UC Berkeley to work on projects involving spectroscopy. A future goal is to enable remote observing with the spectrograph.

One caveat to full remote functionality of the spectrograph is that there is no motor attached to the micrometer for adjustment of the grating. The spectrograph will not be able to change which wavelengths it is observing unless someone is on site at the Leuschner observatory doing the adjustments manually.

6.1 Flip Mirror

A flip mirror is planned for installation on the 30-inch telescope. It has three ports for instruments, and a mirror on a motor which is controlled using a Raspberry Pi.

The flip mirror was previously being used on the Leuschner 30-inch telescope with an infrared camera, but has since been removed and no instruments have been on the telescope besides an imaging camera and the new spectrograph. Since the flip mirror was previously installed on the 30-inch telescope, the flip mirror should be able to go back on it without much alteration.

Appendix A: Dispersion Solutions

These are the dispersion solutions from the IRAF database files for the two dark images used for the wavelength calibration of our spectrum from Vega.

```
# Mon 15:37:05 17-Jun-2019
begin identify 30NEON15-28VEGADARKex.0001 - Ap 1
id 30NEON15-28VEGADARKex.0001
task identify
image 30NEON15-28VEGADARKex.0001 - Ap 1
aperture 1
aplow 1180.24
aphigh 1216.55
units Angstroms
features 5
         187.38 5343.39932  5343.2834   4.0 1 1 NeI
         212.52 5341.14018  5341.0938   4.0 1 1 NeI
         330.19 5330.56641   5330.672   4.0 1 1 NeI
        2717.52 5116.04547  5116.5032   4.0 1 1 NeI
        3109.94 5080.78403   5080.383   4.0 1 1 NeI
```

```
function chebyshev
order 2
sample *
naverage 1
niterate 0
low_reject 3.
high_reject 3.
grow 0.
coefficients 6
1.
2.
187.3803100585938
3109.935546875
5212.091675139452
-131.3076403211365

# Mon 15:31:08 17-Jun-2019
begin identify 60NEON15-28BDARKex.0001 - Ap 1
id 60NEON15-28BDARKex.0001
task identify
image 60NEON15-28BDARKex.0001 - Ap 1
aperture 1
aplow 1180.24
aphigh 1216.55
units Angstroms
features 9
```

```
        185.93  5343.2891  5343.2834   4.0 1 1 NeI
        211.01 5341.09192  5341.0938   4.0 1 1 NeI
        328.66 5330.77122  5330.7775   4.0 1 1 NeI
       1754.63 5203.89424  5203.8962   4.0 1 1 NeI
       1873.80 5193.14141  5193.1251   4.0 1 1 NeI
       1923.87 5188.61667  5188.6122   4.0 1 1 NeI
       2405.18 5144.91381  5144.9384   4.0 1 1 NeI
       2715.85 5116.50522  5116.5032   4.0 1 1 NeI
       3108.36 5080.38923   5080.383   4.0 1 1 NeI
function chebyshev
order 3
sample *
naverage 1
niterate 0
low_reject 3.
high_reject 3.
grow 0.
coefficients 7
1.
3.
185.9300000000001
3108.355224609375
5212.7061356076
-131.4499317888662
-0.8669722116745255
```

Appendix B: Sensitivity Function

This is the sensitivity function output from our IRAF logfile.

```
Fitting function is chebyshev of order 5 with 11 points and RMS of 0.0064.
       Image Airmass  Points    Shift RMS Fit   Dev 1   Dev 2   Dev 3
VegaWavSpec.fits   1.050      11  0.0000  0.0061  0.0012 -0.0013  0.0004


  Lambda     Fit     Avg   Resid  SD Avg     N     Ext    Dext
 5075.00  31.358  31.355 -0.0030  0.0000     1  0.0000  0.0000
 5100.00  31.426  31.431  0.0052  0.0000     1  0.0000  0.0000
 5125.00  31.474  31.475  0.0015  0.0000     1  0.0000  0.0000
 5150.00  31.509  31.511  0.0015  0.0000     1  0.0000  0.0000
 5175.00  31.538  31.525 -0.0136  0.0000     1  0.0000  0.0000
 5200.00  31.563  31.568  0.0044  0.0000     1  0.0000  0.0000
 5225.00  31.586  31.588  0.0023  0.0000     1  0.0000  0.0000
 5250.00  31.603  31.610  0.0071  0.0000     1  0.0000  0.0000
 5275.00  31.613  31.613 -0.0005  0.0000     1  0.0000  0.0000
 5300.00  31.609  31.600 -0.0093  0.0000     1  0.0000  0.0000
 5325.00  31.583  31.588  0.0043  0.0000     1  0.0000  0.0000
```

Appendix C: Data Files

The following is a selection of bright lines from *The Solar Spectrum 2935 Å to 8770 Å: Second Revision of Rowland's Preliminary Table of Solar Spectrum Wavelengths* [18]. This list is formatted for use as a line list in IRAF. The first column contains wavelengths of lines in Angstroms. The second column contains a shortened description of the respective wavelength line. Full descriptions of the lines may be found in the cited text. The file should be saved as plain text with the extension .dat and placed in the linelists folder (iraf/noao/lib/linelists). The line list may then be used with the **identify** task.

```
# units Angstroms
5133.699    FeI
5137.080    NiI
5137.393    FeI
5139.261    FeI
5139.473    FeI
5141.746    FeI
5142.530    FeI
```

5142.936	FeI
5146.491	NiI
5148.237	FeI
5150.852	FeI
5150.938	FeI
5151.917	FeI
5154.075	FeI
5162.281	FeI
5165.415	FeI
5166.284	FeI(CrI)
5167.327	MgI(magnesiumtripletline)
5168.908	FeI
5171.610	FeI
5172.698	MgI(magnesiumtripletline)
5183.619	MgI(magnesiumtripletline)
5188.698	TiII
5188.852	CaI
5191.465	FeI
5192.353	FeI
5192.978	TiI
5194.949	FeI
5195.480	FeI
5196.065	FeI
5195.576	FeII
5198.718	FeI
5202.348	FeI

5215.188	FeI
5216.288	FeI
5217.396	FeI
5226.870	FeI(CrI)
5227.192	FeI
5229.860	FeI
5232.952	FeI
5234.630	FeI
5235.390	FeI
5250.654	FeI
5254.953	CrI-|FeI
5261.708	CaI
5262.248	CaI
5263.314	FeI
5264.160	CrI
5264.246	CaI
5265.560	CaI
5266.563	FeI
5269.550	FeI
5270.269	FeI
5270.383	FeI
5273.170	FeI
5273.389	FeI
5276.002	FeI
5281.798	FeI
5283.629	FeI

5296.702	CrI
5297.385	CrI
5298.023	CrI
5298.283	CrI
5302.307	FeI
5307.369	FeI
5316.620	FeII
5324.191	FeI
5328.051	FeI
5328.542	FeI
5329.147	CrI
5332.908	FeI
5336.794	TiII
5339.937	FeI
5341.033	||FeIMnI(ScI)
5345.807	CrI
5348.326	CrI
5349.469	CaI
5362.867	FeII
5364.880	FeI
5367.476	FeI
5369.974	FeI
5371.501	FeI
5383.380	FeI

The following is a list of neon lines from 5059 Å to 5360 Å retrieved from the

NIST Atomic Spectra Database [12]. This list is formatted for use as a line list in IRAF. This list is formatted for use as a line list in IRAF. The first column contains wavelengths of lines in Angstroms. The second column contains a shortened description of the respective wavelength line. The file should be saved as plain text with the extension .dat and placed in the linelists folder (iraf/noao/lib/linelists). The line list may then be used with the **identify** task.

```
# units Angstroms
5031.3484    NeI
5031.5087    NeI
5036.0016    NeI
5037.5927    NeI
5037.7512    NeI
5041.598
5042.853    NeI
5045.816    NeI
5046.608    NeI
5052.9443    NeI
5059.150    NeI
5074.0459    NeI
5074.2007    NeI
5076.5971    NeI
5078.414    NeII
5078.7693    NeI
5080.3830    NeI
```

5081.360	NeI
5083.9773	NeI
5090.321	NeI
5099.0522	NeI
5099.546	NeII
5104.7011	NeI
5113.6724	NeI
5116.5032	NeI
5117.0246	NeI
5120.5059	NeI
5121.866	NeI
5122.2565	NeI
5122.3613	NeI
5128.280	NeI
5137.150	NeII
5142.80	NeIII
5143.265	NeI
5144.9384	NeI
5145.011	NeI
5145.1351	NeI
5150.0842	NeI
5151.9610	NeI
5154.4271	NeI
5156.6672	NeI
5158.9018	NeI
5163.4847	NeI

5178.508	NeII
5182.320	NeI
5188.6122	NeI
5189.164	NeII
5191.3223	NeI
5193.1251	NeI
5193.2240	NeI
5197.565	NeII
5198.481	NeII
5202.240	NeII
5203.58	NeII
5203.8962	NeI
5206.565	NeI
5208.8648	NeI
5210.5672	NeI
5212.363	NeII
5213.339	NeII
5214.3389	NeI
5218.268	NeII
5222.3517	NeI
5231.523	NeII
5234.0271	NeI
5234.637	NeII
5235.867	NeII
5245.834	NeII
5263.123	NeII

5274.0393	NeI
5280.0853	NeI
5280.3	NeVI
5282.9	NeVI
5287.2	NeVI
5289.9	NeVI
5298.1891	NeI
5304.7580	NeI
5314.7851	NeI
5316.8046	NeI
5320.550	NeI
5326.3960	NeI
5330.6720	NeI
5330.7775	NeI
5333.3083	NeI
5335.710	NeI
5341.0938	NeI
5342.700	NeI
5343.0048	NeI
5343.2834	NeI
5349.2038	NeI
5353.513	NeI
5355.1640	NeI
5355.3394	NeI
5355.4236	NeI
5358.020	Ne

The following is a file formatted for use with the **standard** task containing data on the energy distribution of Vega between 4975 Å to 5575 Å, from *Stellar Absolute Fluxes and Energy Distributions from 0.32 to 4.0μm* by D. S. Hayes [8]. The file should be saved as plain text with a .dat extension. This file must be placed in a folder within the onedstds folder (iraf/noao/lib/onedstds).

```
# VEGA
4975. -0.015 25.
5000. 0.000 25.
5025. 0.017 25.
5050. 0.034 25.
5075. 0.048 25.
5100. 0.064 25.
5125. 0.079 25.
5150. 0.095 25.
5175. 0.110 25.
5200. 0.126 25.
5225. 0.139 25.
5250. 0.154 25.
5275. 0.167 25.
5300. 0.183 25.
5325. 0.192 25.
5350. 0.206 25.
5375. 0.221 25.
5400. 0.234 25.
5425. 0.249 25.
5450. 0.264 25.
```

5475.	0.278	25.
5500.	0.296	25.
5525.	0.311	25.
5550.	0.324	25.
5575.	0.333	25.

Appendix D: Additional Objects Observed and Raw Images

Object	Time Observed	Leuschner RA	Leuschner Dec	Focus
Vega (α Lyrae)	21:53	18:36:00	38:50:30	24075
Arcturus (α Boötis)	23:00	14:15:06	19:09:34	Unchanged
Jupiter	23:10	17:14:37.6	-22:23:26	23747.8
Alioth (ϵ Ursae Majoris)	23:39	12:53:21	55:57:00	Unchanged
Vega (α Lyrae)	00:06	18:36:04.5	38:47:46	24024.8
Arcturus (α Boötis)	00:31	14:15:09	19:09:34	Unchanged
Vega (α Lyrae)	02:17	18:36:04.5	38:47:46	Unchanged
Arcturus (α Boötis)	02:31	14:15:09	19:09:34	Unchanged
Jupiter	02:44	Unknown	Unknown	Unchanged

Table 6.1: List of objects observed the evening of June 6th, 2019 and on the morning of June 7th, 2019. Times are local to the observatory (PDT). Slewing to the right ascension and declination values given placed the objects in the field of view of the guide camera around the given times.

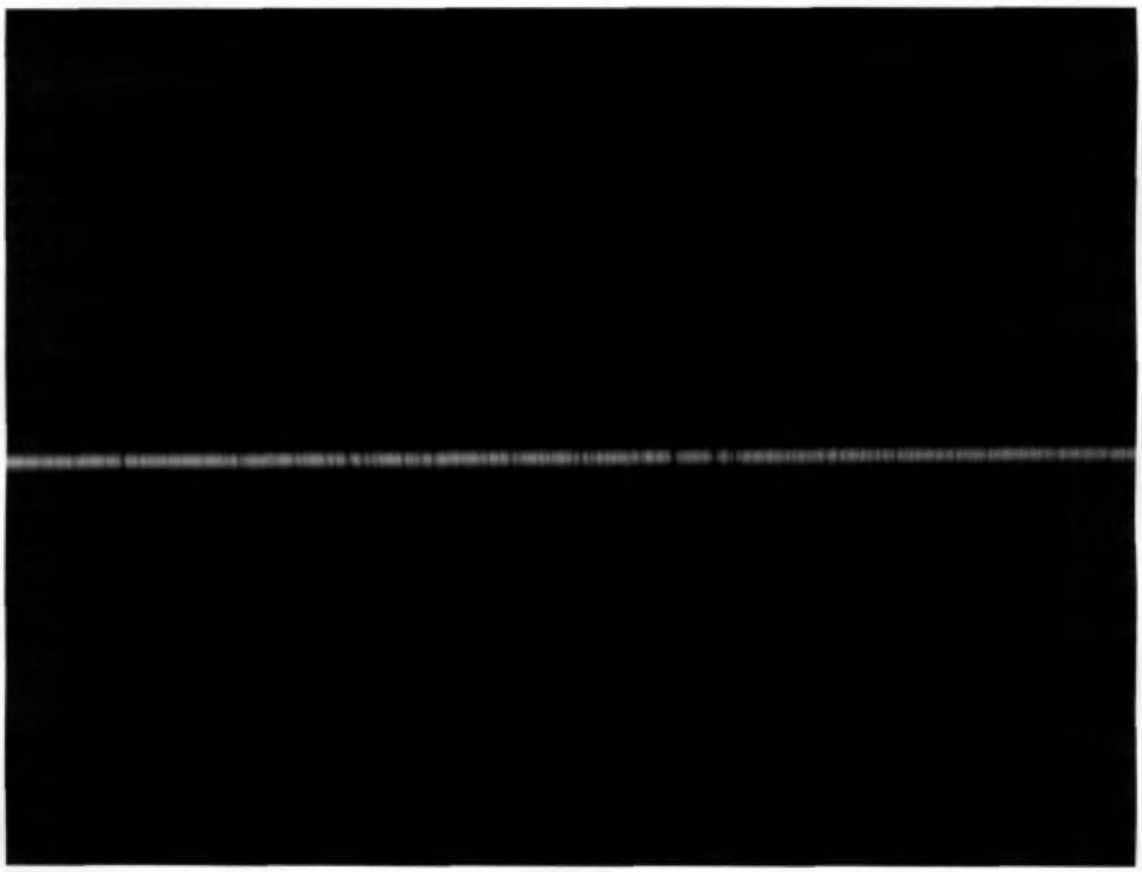

Figure 6.1: 60 second exposure of Arcturus on June 7, 2019 at 2:33 am PDT. DS9 scale parameters: Low = 925, High = 65535

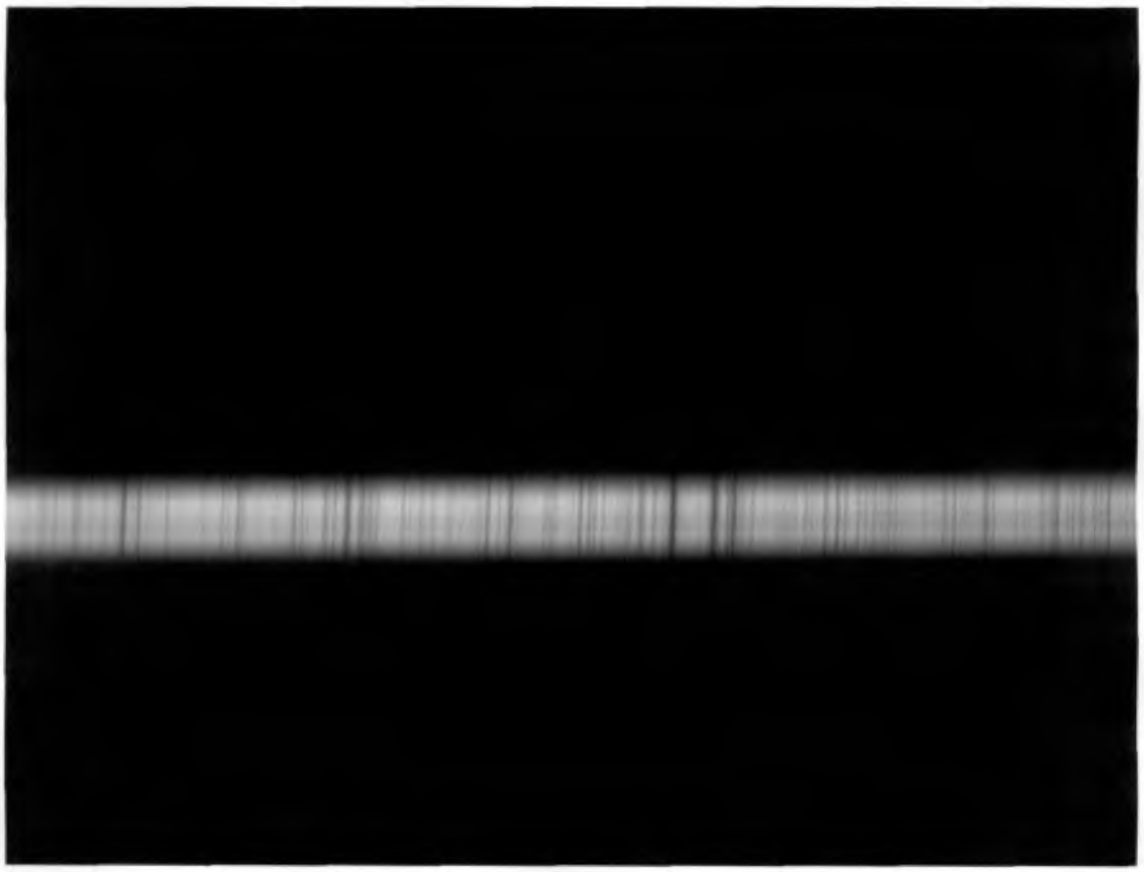

Figure 6.2: 60 second exposure of Jupiter on June 7, 2019 at 2:44 am PDT. DS9 scale parameters: Low = 925, High = 65535

Bibliography

[1] UC Berkeley Astronomy, *Optics the leuschner thirty inch telescope*, `http://ugastro.berkeley.edu/leuschner/thirty/optics/index.html`, Retrieved May 22, 2017.

[2] UC Berkeley Astronomy, *Leuschner observatory*, `http://ugastro.berkeley.edu/leuschner/old_site/index.html`, December 2005, Retrieved April 9, 2019.

[3] B. W. Carroll, *An introduction to modern astrophysics*, Addison-Wesley, San Francisco, CA, 2007.

[4] F. R. Chromey, *To measure the sky: An introduction to observational astronomy*, Cambridge University Press., Cambridge, UK, 2011.

[5] A. Fries, *Commissioning the refurbished leuschner 30-in telescope and observing the sun-grazing comet ison*, San Francisco State University, San Francisco, CA, December 2014.

[6] E. C. Gonzales, *Commissioning the refurbished 30-inch leuschner telescope and testing its exoplanet detection capabilites*, San Francisco State University, San Francisco, CA, January 2015.

[7] Santa Barbara Imaging Group, *Model st-8300m/c ccd camera operating manual*, `https://diffractionlimited.com/wp-content/uploads/2016/03/ST-8300-Manual_12.pdf`, December 2009, Retrieved June 21, 2019.

[8] D. S. Hayes, *Stellar absolute fluxes and energy distributions from 0.32 to 4.0 μm.*, Calibration of Fundamental Stellar Quantities (D. S. Hayes, L. E.

Pasinetti, and A. G. D. Philip, eds.), IAU Symposium, vol. 111, Jan 1985, pp. 225–252.

[9] Shelyak Instruments, *Lhires iii user guide*, `https://www.shelyak.com/wp-content/uploads/DC0004A-Lhires-III-User-Guide-English-1.pdf`, December 2006.

[10] I. R. King, *Leuschner Observatory, University of California, Berkeley, California. Report 1967-1968.*, Bulletin of the American Astronomical Society, Bulletin of the American Astronomical Society, vol. 1, January 1969, pp. 36–44.

[11] C. Kitchin, *Telescopes and techniques: An introduction to practical astronomy*, Springer, London, UK, 2003.

[12] A. Kramida, Yu. Ralchenko, J. Reader, and NIST ASD Team, NIST Atomic Spectra Database (ver. 5.6.1), [Online]. Available: `https://physics.nist.gov/asd` [2019, June 17]. National Institute of Standards and Technology, Gaithersburg, MD., 2018.

[13] A. O. Leuschner, *History and Aims of the Students' Observatory*, Publications of the Astronomical Society of the Pacific **16** (1904), 68.

[14] Diffraction Limited, *Legacy product support*, `https://diffractionlimited.com/support/sbig-archives/`, 2019, Retrieved June 24, 2019.

[15] Starlight Xpress Ltd., *Downloads*, `https://www.sxccd.com/drivers-downloads`, Retrieved June 24, 2019.

[16] Starlight Xpress Ltd., *Ultrastar handbook issue 1*, `https://www.sxccd.com/handbooks/Handbook%20for%20the%20Ultrastar.pdf`, August 2015.

[17] P. Massey, F. Valdes , and J. . Barnes, *A User's Guide to Reducing Slit Spectra with IRAF*, http://www.astro.iag.usp.br/~jorge/aga5802/spect_iraf_reducao.pdf, April 1992.

[18] C. E. Moore, M. G. J. Minnaert, and J. . Houtgast, *The solar spectrum 2935 Å to 8770 Å: Second revision of rowland's preliminary table of solar spectrum wavelengths*, United States Department of Commerce: National Bureau of Standards, Washington, D.C., December 1966.

[19] San Francisco State University Department of Physics and Astronomy, *Leuschner*, `http://www.physics.sfsu.edu/observatory/leuschner.html`, Retrieved February 1, 2019.